Structure and Phase Transition in $(C_2H_5NH_3)_3Sb_2Cl_9 \cdot (C_2H_5NH_3)SbCl_4$; X-ray, DSC and Dielectric Studies

Maciej Bujak and Jacek Zaleski

Institute of Chemistry, University of Opole, Oleska 48, 45 052 Opole, Poland

Reprint requests to Prof. J. Z.; Fax: ++48 77 4410741; E-mail: zaleski@uni.opole.pl

Z. Naturforsch. **55 a,** 526–532 (2000); received January 10, 2000

The structure of $(C_2H_5NH_3)_3Sb_2Cl_9 \cdot (C_2H_5NH_3)SbCl_4$ at 295 K has been determined. The crystals are orthorhombic, space group $Pna2_1$ (a = 16.925(3), b = 24.703(5), c = 7.956(2) Å, V = 3326.4(12) Å^3, Z = 4, d_c = 2.018, d_m = 2.01(1) Mg m^{-3}). They consist of an anionic sublattice composed of two different polymeric zig-zag chains. One is built of $Sb_2Cl_9^{3-}$ units (corner sharing octahedra) and the other one is made of corner sharing $SbCl_5^{2-}$ square pyramids. In the cavites between the polyanionic chains four non-equivalent ethylammonium cations are located. Three of them are disordered. The cations are connected to the anions by weak N-H...Cl hydrogen bonds. A first order phase transition of the order-disorder type was found at 274 K. It was studied by DSC, dielectric and X-ray diffraction methods. The mechanism of the phase transition is attributed to the ordering of at least one of the ethylammonium cations.

Key words: Ethylamine; Chloroantimonate(III); Structure; Phase Transition.

1. Introduction

Halogenoantimonates(III) with organic cations have widely been investigated. They show numerous phase transitions, some of them to polar phases. These compounds have anionic sublattices composed, generally, of $SbCl_6^{3-}$ deformed octahedra, isolated or connected with each other by corners, edges or faces, forming various polyanionic units. There exists literature on halogenoantimonates(III), most of them involving properties of methyl-, dimethyl-, trimethyl- and tetramethylammonium derivatives: [1 - 4].

The characteristic feature of this family of compounds is that antimony(III) shows a tendency towards distorted octahedral coordination, with the Sb-X (X = Cl, Br, I) bond lengths differing significantly from one another. This is attributed to the deviation from spherical symmetry of the spatial distribution of the lone electron pair located at Sb(III).

The present work is part of a larger project of studying the crystal structure and phase transitions of halogenoantimonates(III). The main focus in those investigations is directed to the crystallochemistry of Sb(III) compounds and their physical properties.

Ethylammonium chloroantimonates(III) were reported to crystallize in two different stoichiometries: $(C_2H_5NH_3)SbCl_4$ and $(C_2H_5NH_3)_3SbCl_6$ [5 - 6]. Only the structure of the second compound was reported so far. We describe here the crystal structure and phase transition of a salt with the general formula $(C_2H_5NH_3)_4Sb_3Cl_{13}$. It is the first report on the structure of a salt with this stoichiometry. Since its anionic sublattice is built of two different polymeric zig-zag chains characteristed by two different stoichiometries, ($R_3Sb_2Cl_9$ and $RSbCl_4$) [7 - 8], we shall use the formula $(C_2H_5NH_3)_3Sb_2Cl_9 \cdot (C_2H_5NH_3)SbCl_4$.

2. Experimental Details

The $(C_2H_5NH_3)_3Sb_2Cl_9 \cdot (C_2H_5NH_3)SbCl_4$ crystals were synthesised in a reaction of ethylamine and antimony trichloride (molar ratio from 1:2 to 2:1) in water solution of hydrochloric acid. Transparent, needle-shaped crystals were grown by slow evaporation at room temperature. Their melting point is at 425 - 429 K.

Data for the structure determination were collected on a KUMA KM-4 κ-axis diffractometer with Mo Kα radiation (λ = 0.71073 Å; graphite monochromator). Lattice parameters were refined from setting angles of 24 reflections in the $13° < 2\theta < 27°$ range. A total of 4090 reflections with $4° < 2\theta < 55.6°$ were collected

0932–0784 / 00 / 0500–0526 $ 06.00

Table 1. Crystal data and structure determination summary for $(C_2H_5NH_3)_3Sb_2Cl_9 \cdot (C_2H_5NH_3)SbCl_4$.

Crystal data	
Empirical formula	$C_8H_{32}Cl_{13}N_4Sb_3$
Colour; habit	Colourless; needles
Crystal size	0.34×0.30×0.28 mm
Crystal system	Orthorhombic
Space group	$Pna2_1$
Unit cell dimensions	a = 16.925(3) Å
	b = 24.703(5) Å
	c = 7.956(2) Å
Volume	3326.4(12) Å^3
Z	4
Formula weight	1010.48
Density (calculated)	2.018 Mg·m^{-3}
Density (measured)	2.01(1) Mg·m^{-3}
Absorption coefficient	3.47 mm^{-1}
Temperature	295(2) K
Data collection	
Diffractometer/scan	KUMA KM-4/ω-θ
Radiation	Mo Kα (λ = 0.71073 Å)
θ range	2 - 27.8°
Index ranges	$0 \le h \le 22$; $0 \le k \le 29$; $-10 \le l \le 0$
Independent reflections	4089
Observed reflections [$I > 2\sigma(I)$]	2131
Solution and refinement[a]	
System used	SHELX-97
Solution	Patterson method
Refinement method	Full-matrix least-squares
Correction applied	Lorentz; polarization; absorption
Refined parameters	343
Final R indexes [$I > 2\sigma(I)$]	R = 3.19%, wR = 7.93%
wR (all data)	10.07%
Goodness of fit	1.001
Flack parameter	–0.08(12)
Largest diff. peak and hole	0.74/–0.74 eÅ^{-3}

[a] Weight scheme: $w = 1/[\sigma^2(F_0^2) + (0.0421P)^2 + 0.5839P]$ where $P = (F_0^2 + 2F_c^2)/3$

Table 2. Atomic coordinates (x10^4) and equivalent isotropic displacement parameters (Å^2×10^3) for non-H atoms. U_{eq} is defined as one third of the trace of the orthogonalized U_{ij} tensor. For the numbering of the atoms cf. Figure 3.

Atom	x	y	z	U_{eq}
Sb1	5201(1)	828(1)	6721(1)	54(1)
Sb2	8057(1)	564(1)	6707(1)	47(1)
Sb3	10074(1)	1526(1)	1717(1)	48(1)
Cl1	3810(1)	820(1)	6698(4)	65(1)
Cl2	5132(1)	1522(1)	4515(2)	81(1)
Cl3	5222(1)	1510(1)	8957(2)	102(1)
Cl4a	5127(1)	111(1)	9516(3)	90(1)
Cl4b	4937(2)	–119(1)	9005(5)	103(1)
Cl5	7165(1)	1343(1)	6647(6)	91(1)
Cl6	7253(1)	142(1)	8933(2)	93(1)
Cl7	7207(1)	150(1)	4531(1)	93(1)
Cl8a	9096(2)	1142(1)	4464(3)	98(1)
Cl8b	8883(2)	945(1)	3964(4)	114(1)
Cl9	9034(1)	1079(1)	9127(2)	108(1)
Cl10	9055(1)	–413(1)	6718(5)	83(1)
Cl11	10913(1)	1884(1)	–418(2)	93(1)
Cl12	9270(1)	2323(1)	1670(5)	94(1)
Cl13	10863(1)	1910(1)	3998(2)	90(1)
N1	9422(2)	2267(1)	6764(11)	120(1)
C1	8692(2)	2458(2)	7325(5)	101(2)
C2	8133(2)	2669(2)	6092(6)	128(2)
N2	6168(2)	–766(1)	6737(16)	98(1)
C3a	6537(4)	–1258(2)	6620(3)	84(1)
C4a	7219(5)	–1375(3)	7292(11)	89(1)
C3b	6897(5)	–1166(3)	6017(11)	89(1)
C4b	7062(6)	–1525(3)	7537(12)	97(1)
N3a	6871(4)	1084(1)	11878(15)	139(3)
C5a	7100(6)	1607(2)	12264(6)	116(3)
C6a	6990(6)	2012(2)	10913(7)	116(3)
N3b	6507(3)	1039(2)	11430(11)	110(2)
C5b	7199(3)	1354(2)	11442(16)	121(2)
C6b	7069(5)	1948(2)	11517(15)	127(3)
N4a	9192(4)	–85(2)	10942(8)	100(2)
C7a	9119(2)	–612(2)	11549(12)	83(2)
C8a	8300(3)	–818(3)	11790(2)	112(2)
N4b	9471(3)	–320(3)	10728(6)	96(2)
C7b	8921(3)	–374(2)	12028(7)	91(2)
C8b	8338(3)	–823(2)	11861(19)	105(2)

using the ω-θ scan technique. Out of 4089 independent reflections, 2131 had $I > 2\sigma$ (I). Two control reflections measured after an interval of 50 reflections show that the intensity variation was negligible. Lorentz, polarisation and semiempirical absorption correction (via ψ-scans, based on reflection measurements at different azimuthal angles [9]) were applied (T_{min} = 0.385, T_{max} = 0.443).

The structure was solved by the Patterson method and refined by a full-matrix least squares method. From the systematic absences, a centrosymmetric Pnma and a non-centrosymmetric $Pna2_1$ space group follows. An attempt to refine the structure in the centrosymmetric space group led to an unreasonable model of disorder. Therefore the $Pna2_1$ group was selected (Flack parameter = –0.08(12)). The second enantiomer was checked. The final R indices are comparable to those for the first one, with the absolute structure parameter equal to 0.38(11). Parameters of non-hydrogen atoms were refined using anisotropic temperature factors. The occupancy factors for all split atoms (Cl, N, C) were refined until converged and then were fixed at 0.5. All hydrogen atoms were included using standard geometric criteria. Hydrogen atoms of methyl and methylene groups were constrained to distances of 0.96 Å (H atoms of amine

group to 0.90 Å). The positions of hydrogen atoms were refined using the riding model.

KUMA software was used in the data collection, cell refinement and data reduction processes [10]. The SHELX-97 [11] program was used for structure solution and refinement. The structure drawings were prepared using the SHELXTL program [9]. The details of the data collection and processing are listed in Table 1. Final atomic coordinates and equivalent isotropic displacement parameters for non-H atoms are shown in Table 2 (For the numbering of the atoms cf. Figure 3). A list of calculated and observed structure factors may be obtained from the authors on request.

The differential scanning calorimetry (DSC) studies were carried out on a Perkin-Elmer DSC-7 calorimeter with a cooling/heating rate of 20 and 10 K min^{-1}. The measurements were performed at 100 - 470 K.

The complex electric permittivity was measured along the *c* direction (perpendicular to the cleavage plane) by an HP4284A precision LCR meter in the frequency range 75 kHz - 30 MHz. The measurements were performed at 120 - 320 K. The temperature was changed at the rate 0.2 K min^{-1} in the vicinity of the phase transition and about 0.5 K min^{-1} elsewhere. The dimensions of the measured plates were about 4 × 3 × 1 mm^3. The plates were silver painted before the experiment. No dielectric dispersion was observed in the studied frequency range. The over-all error of the real part of the complex electric permittivity was smaller than 10%.

The temperature dependence of the lattice parameters was measured on the KM-4 KUMA diffractometer with the Oxford Cryosystem cooler (dry nitrogen-gas stream, temperature stability 0.1 K). The measurements were carried out at 140 - 300 K. Lattice parameters were refined from setting angles of 20 reflections in the $13° < 2\theta < 21°$ range.

3. Results and Discussion

3.1. X-ray Studies

In $(C_2H_5NH_3)_3Sb_2Cl_9 \cdot (C_2H_5NH_3)SbCl_4$ crystals each antimony atom is surrounded by six chlorine atoms. Three of them form much shorter Sb-Cl bonds than the others. The shorter Sb-Cl distances are in the range: 2.355(1) - 2.472(1) Å, while the longer ones

Table 3. Selected bond lengths [Å] for $(C_2H_5NH_3)_3Sb_2Cl_9 \cdot (C_2H_5NH_3)SbCl_4$.

Sb1-Cl1	2.355(1)	Sb1-Cl2	2.457(1)
Sb1-Cl3	2.450(2)	Sb1-Cl4a	2.845(3)
Sb1-Cl4a^{I}	2.960(3)	Sb1-Cl4b	2.996(3)
Sb1-Cl4b^{I}	2.790(3)	Sb2-Cl5	2.446(1)
Sb2-Cl6	2.465(1)	Sb2-Cl7	2.472(1)
Sb2-Cl8a	2.883(3)	Sb2-Cl8b	2.758(3)
Sb2-Cl9	2.840(2)	Sb2-Cl10	2.945(1)
Sb3-Cl8a	2.902(3)	Sb3-Cl8b	3.052(3)
Sb3-Cl9^{II}	2.925(2)	Sb3-Cl10^{III}	3.120(1)
Sb3-Cl11	2.385(1)	Sb3-Cl12	2.395(1)
Sb3-Cl13	2.445(2)		

Symmetry codes: (^{I}) $-x + 1, -y, z - 1/2$; (^{II}) $x, y, z - 1$; (^{III}) $-x + 2, -y, z - 1/2$.

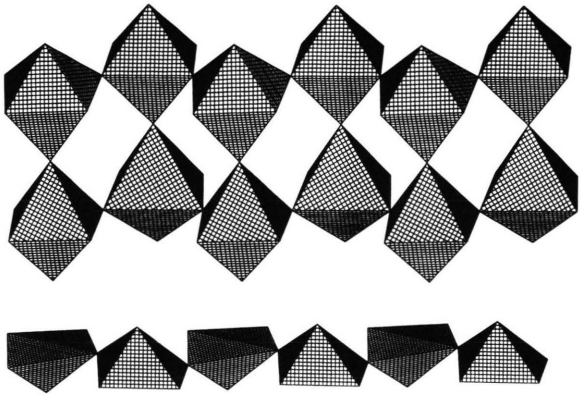

Fig. 1. The anionic sublattice of $(C_2H_5NH_3)_3Sb_2Cl_9 \cdot (C_2H_5NH_3)SbCl_4$ in polyhedral representation. Polymeric one dimensional zig-zag chains are extended along the *c* axis, *top:* $(Sb_2Cl_9^{3-})_n$, *bottom:* $(SbCl_4^{-})_n$.

are between: 2.758(3) and 3.120(1) Å. An exception is the longest Sb1-Cl5 distance, which amounts to 3.559(1) Å. The environment of an Sb1 atom may therefore be treated either as a much deformed octahedron (according to Pauling the sum of the van der Waals radii for Sb(III) and Cl is 4.0 Å [12]) or a square pyramid. Considering, however, the significant difference between the longest Sb-Cl bonds and the length of Sb1-Cl5 contact (ca. 0.44 Å) together with the large deviation of Cl-Sb-Cl angles involving Cl5 from 90° we decided to treat the environment of the Sb1 atom as a square pyramid, rather than a much distorted octahedron.

The anionic sublattice of $(C_2H_5NH_3)_3Sb_2Cl_9 \cdot (C_2H_5NH_3)SbCl_4$ salt is composed of two independent polyanionic chains, extended along the *c*-axis; one composed of $Sb_2Cl_9^{3-}$ and the other one of $SbCl_4^{-}$ units. It should be noted that the title crystal

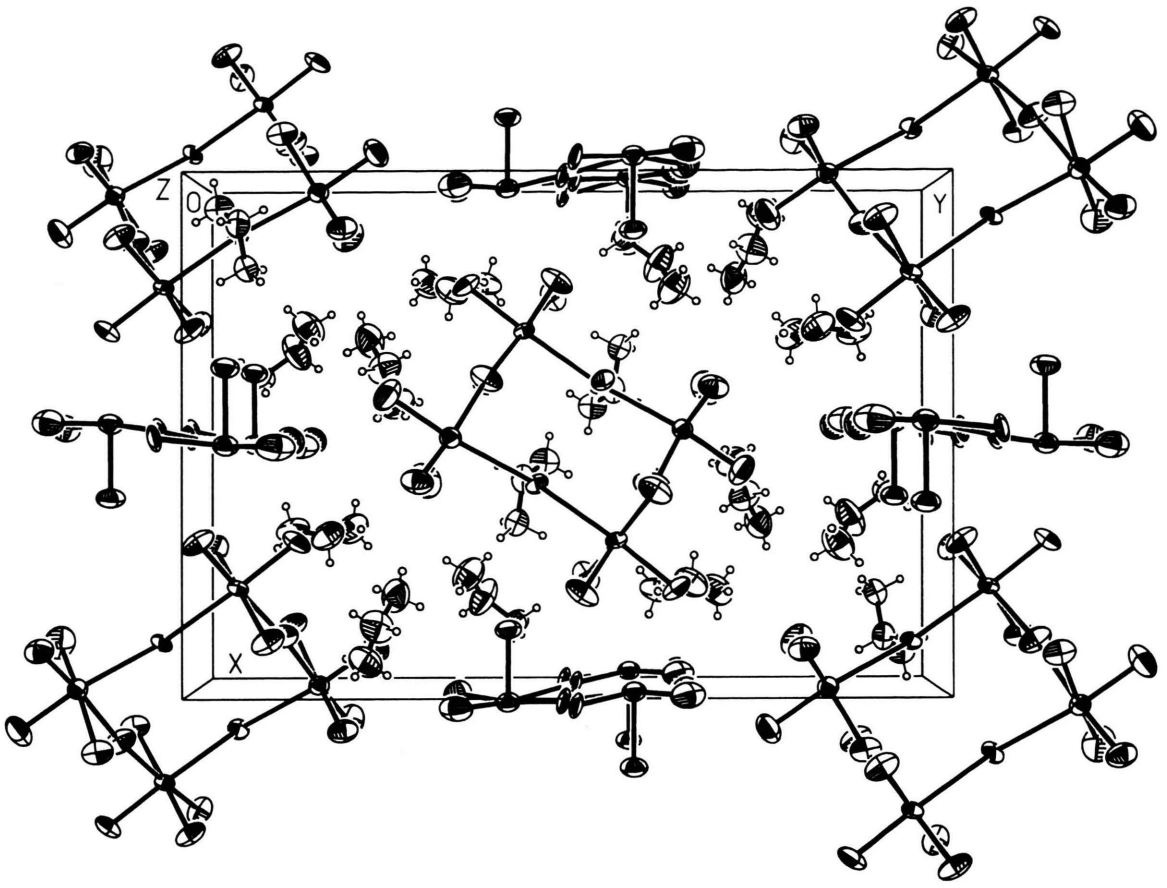

Fig. 2. Packing diagram of $(C_2H_5NH_3)_3Sb_2Cl_9 \cdot (C_2H_5NH_3)SbCl_4$. Only one position of disordered atoms is shown for clarity. Displacement ellipsoids are at 50% probability.

appears to be the first alkylammonium halogenoantomonate(III) in which the anionic part of the structure is composed of two independent subunits, characteristic of two different stoichiometries.

The $(Sb_2Cl_9^{3-})_n$ double chain consists of $SbCl_6^{3-}$ octahedra connected by the corners in such a way that each antimony atom is surrounded by three bridging and three terminal chlorine atoms (Figure 1 (top)). The other polyanionic chain $(SbCl_4^-)_n$ is built of corner sharing $SbCl_5^{2-}$ square pyramids (Figure 1 (bottom)). Two of thirteen independent chlorine atoms are disordered and split between two sites. The bond lengths and angles within the anionic sublattice are given in Tables 3 and 4. A packing plot of the unit cell is shown in Figure 2.

In the $(SbCl_4^-)_n$ chain built of square pyramids, the Sb-Cl bond lengths fall into the range 2.355(1) - 2.996(3) Å. The bridging chlorines possess the longest Sb-Cl bonds (2.790(3) - 2.996(3) Å), the axial ones the shortest (2.355(1) Å), while two other equatorial bonds have intermediate lengths (2.450(2) - 2.457(1) Å). Two of the bridging chlorine atoms are disordered. They are split between two sites, with half occupancy (Cl4a, Cl4b and $Cl4a^I$, $Cl4b^I$) (Figure 3). The Cl-Sb-Cl angles, cis to each other, range from 73.73(8) to 102.19(8)°.

The chain built of square pyramids connected with each other by corners was also found in $[(C_2H_5)_3NH]SbCl_4$ [8]. The bond lengths in this crystal are similar to those of the title compound. The equatorial Sb-Cl bonds fall in the range 2.433(2) - 2.942(2) Å, whereas two independent axial bond-lengths are 2.381(1) and 2.388(1) Å. A significant difference, however, is found in the geometry of the polyanionic chain. The angle between the planes defined by the equatorial chlorines of adjacent

Table 4. Selected bond angles [°] for $(C_2H_5NH_3)_3Sb_2Cl_9 \cdot (C_2H_5NH_3)SbCl_4$.

Cl1-Sb1-Cl2	87.31(7)	Cl7-Sb2-Cl8a	97.23(7)
Cl1-Sb1-Cl3	91.46(7)	Cl7-Sb2-Cl8b	83.21(7)
Cl1-Sb1-Cl4a	87.50(8)	Cl7-Sb2-Cl9	177.65(5)
Cl1-Sb1-Cl4a^{I}	78.55(7)	Cl7-Sb2-Cl10	89.83(6)
Cl1-Sb1-Cl4b	81.32(8)	Cl8a-Sb2-Cl9	80.95(6)
Cl1-Sb1-Cl4b^{I}	84.54(10)	Cl8a-Sb2-Cl10	93.29(7)
Cl2-Sb1-Cl3	92.26(4)	Cl8b-Sb2-Cl9	95.06(7)
Cl2-Sb1-Cl4a	172.16(6)	Cl8b-Sb2-Cl10	89.48(8)
Cl2-Sb1-Cl4a^{I}	96.59(7)	Cl9-Sb2-Cl10	91.76(6)
Cl2-Sb1-Cl4b	166.29(7)	Cl8a-Sb3-Cl9^{II}	93.67(6)
Cl2-Sb1-Cl4b^{I}	83.16(8)	Cl8a-Sb3-Cl10^{III}	88.92(7)
Cl3-Sb1-Cl4a	82.00(7)	Cl8a-Sb3-Cl11	176.26(6)
Cl3-Sb1-Cl4a^{I}	166.29(6)	Cl8a-Sb3-Cl12	87.50(9)
Cl3-Sb1-Cl4b	95.65(8)	Cl8a-Sb3-Cl13	83.08(7)
Cl3-Sb1-Cl4b^{I}	174.04(8)	Cl8b-Sb3-Cl9^{II}	80.68(7)
Cl4a-Sb1-Cl4a^{I}	88.13(2)	Cl8b-Sb3-Cl10^{III}	84.12(7)
Cl4a-Sb1-Cl4b^{I}	102.19(8)	Cl8b-Sb3-Cl11	170.07(7)
Cl4b-Sb1-Cl4a^{I}	73.73(8)	Cl8b-Sb3-Cl12	91.17(8)
Cl4b-Sb1-Cl4b^{I}	88.14(2)	Cl8b-Sb3-Cl13	96.22(7)
Cl5-Sb2-Cl6	90.34(8)	Cl9^{II}-Sb3-Cl10^{III}	87.24(6)
Cl5-Sb2-Cl7	87.28(8)	Cl9^{II}-Sb3-Cl11	89.80(5)
Cl5-Sb2-Cl8a	88.56(8)	Cl9^{II}-Sb3-Cl12	87.56(8)
Cl5-Sb2-Cl8b	91.66(10)	Cl9^{II}-Sb3-Cl13	176.11(5)
Cl5-Sb2-Cl9	91.17(8)	Cl10^{III}-Sb3-Cl11	92.65(6)
Cl5-Sb2-Cl10	176.75(5)	Cl10^{III}-Sb3-Cl12	173.49(3)
Cl6-Sb2-Cl7	90.40(4)	Cl10^{III}-Sb3-Cl13	94.81(6)
Cl6-Sb2-Cl8a	172.22(7)	Cl11-Sb3-Cl12	91.26(8)
Cl6-Sb2-Cl8b	173.21(7)	Cl11-Sb3-Cl13	93.40(4)
Cl6-Sb2-Cl9	91.38(5)	Cl12-Sb3-Cl13	90.15(8)
Cl6-Sb2-Cl10	88.18(6)		

Symmetry codes: (^{I}) $-x + 1, -y, z - 1/2$; (^{II}) $x, y, z - 1$; (^{III}) $-x + 2, -y, z - 1/2$.

pyramids in the title crystal is 176°, whereas in $[(C_2H_5)_3NH]SbCl_4$ it is only 63°.

In the $(Sb_2Cl_9^{3-})_n$ double chain each antimony atom (Sb2 and Sb3) is bonded to six chlorine atoms with bond lengths between 2.446(1) and 2.945(1) Å for the Sb2 octahedron, and from 2.385(1) to 3.120(1) Å for the Sb3 octahedron. One out of six bridging chlorine atoms (Cl8) is disordered. It is positioned on two sites with occupancy factors of 0.5. All Sb-Cl bonds fall into two clearly defined ranges: 2.385(1) - 2.472(1) Å characteristic of terminal chlorine atoms and 2.758(3) - 3.120(1) Å characteristic of bridging ones. The bond angles for Cl atoms cis to one another are in the range 80.68(7) - 97.23(7)°, significantly deviating from 90°. The N...Cl contacts range from 3.155(7) to 3.385(7) Å, indicating that cations are bound to the anionic sublattice by weak N-H...Cl hydrogen bonds (Table 5).

Table 5. The H-bonds geometry [Å,°] in $(C_2H_5NH_3)_3Sb_2Cl_9 \cdot (C_2H_5NH_3)SbCl_4$.

D-H...A	D-H	H...A	D...A	D-H...A
N1-H1b...Cl8a	0.90	2.48	3.373(6)	170.3
N2-H2a...Cl4a^{I}	0.90	2.44	3.247(8)	149.5
N2-H2c...Cl6	0.90	2.57	3.385(7)	151.0
N31-H31a...Cl7^{IV}	0.90	2.30	3.177(8)	165.7
N32-H32c...Cl3	0.90	2.32	3.155(7)	153.6
N42-H42a...Cl10^{V}	0.90	2.30	3.180(6)	165.1

Symmetry codes: (^{I}) $-x + 1, -y, z - 1/2$; (^{IV}) $x, y, z + 1$; (^{V}) $-x + 2, -y, z + 1/2$.

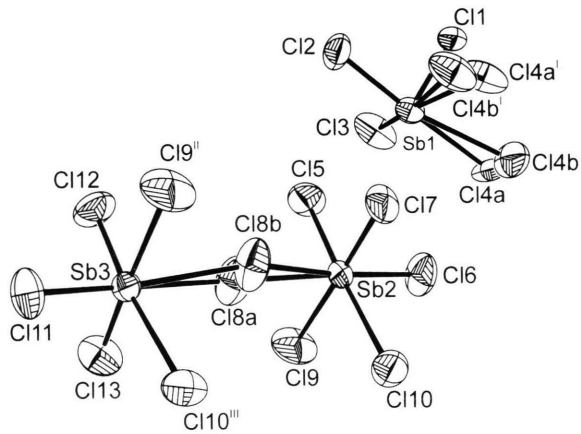

Fig. 3. View of the inorganic part of $(C_2H_5NH_3)_3Sb_2Cl_9 \cdot (C_2H_5NH_3)SbCl_4$ showing the numbering of the Sb and Cl atoms. Displacement ellipsoids are at 50% probability. Symmetry codes: (^{I}) $-x + 1, -y, z - 1/2$; (^{II}) $x, y, z - 1$; (^{III}) $-x + 2, -y, z - 1/2$.

The anionic sublattice, composed of $(Sb_2Cl_9^{3-})_n$ one-dimensional double chains, possess e.g. $(n\text{-}C_3H_7NH_3)_3Sb_2Cl_9$ [7]. Two ranges of Sb-Cl bond lengths were also found in this crystal. The terminal bond lengths are between 2.414(7) and 2.512(7) Å, and the bridging ones between 2.760(9) and 3.025(12) Å.

There are four non-equivalent ethylammonium cations in the crystal structure. They are characterised by large thermal motions, which is reflected in their large temperature factors. Three cations are disordered. The disorder is realised by splitting all atoms between two sites with half occupancy. Freezing the reorientations of cations by lowering the temperature or increasing the pressure may lead to phase transitions.

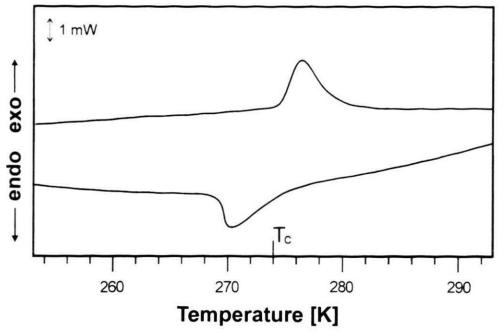

Fig. 4. The DSC curves for $(C_2H_5NH_3)_3Sb_2Cl_9$ $(C_2H_5NH_3)SbCl_4$ recorded on heating and cooling.

3.2. Phase Transition

3.2.1. Differential scanning calorimetry measurements

The DSC curves during cooling and heating for $(C_2H_5NH_3)_3Sb_2Cl_9 \cdot (C_2H_5NH_3)SbCl_4$ in the temperature range 253 - 293 K are presented in Figure 4. The plot reveals one distinct thermal anomaly at ca. 274 K. The enthalpy and entropy of the transition are $\Delta H = 1.52$ kJ mol^{-1} and $\Delta S = 5.61$ J mol^{-1} K^{-1}, respectively. The relatively sharp peak on a DSC curve, the value of the thermal hysteresis and the transition entropy (close to R ln 2 = 5.76 J mol^{-1} K^{-1}) indicate that the phase transition is of first order and of the order-disorder type. It is probably connected with freezing the reorientation motions of at least one of the ethylammonium cations on lowering temperature.

3.2.2. Dielectric studies

Figure 5 presents the temperature dependence of the real part of the electric permittivity (ε') in the vicinity of the phase transition, measured along the *c*-axis at 1 MHz for $(C_2H_5NH_3)_3Sb_2Cl_9 \cdot (C_2H_5NH_3)SbCl_4$. The anomaly was well reproducible, with a thermal hysteresis of ca. 3 K. In the vicinity of the phase transition (+/–1 K) we observed a decrease of the electric permittivity on decreasing the temperature. This supports the supposition that this phase transition is associated with freezing of reorientation motions of the cationic sublattice.

3.2.3. Thermal expansion studies

The lattice parameters *a*, *b*, and *c* of the title compound are plotted as a function of temperature in Figure 6. One anomaly is visible in the range 270 - 278 K,

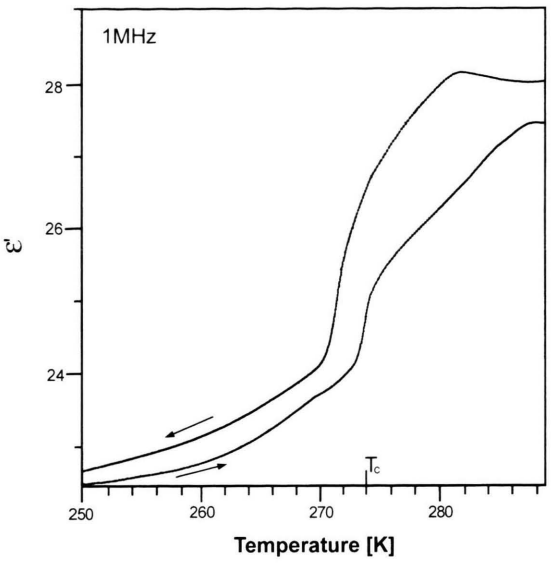

Fig. 5. Temperature dependence of the real part of the electric permittivity for $(C_2H_5NH_3)_3Sb_2Cl_9 \cdot (C_2H_5NH_3)SbCl_4$ crystal along the *c*-axis at 1 MHz.

corresponding to the phase transition found by DSC and dielectric studies. On decreasing temperature the *a* and *c* lattice parameters decrease, while the *b* parameter increases. Below the phase transition temperature we found a broadening and then splitting of the reflections, which indicates that the symmetry of the crystal below T_c is lowered, with change of the crystal system, to monoclinic or triclinic. This prevented us from determining the crystal structure of the title compound below T_c.

4. Conclusions

- The crystal structure of $(C_2H_5NH_3)_3Sb_2Cl_9 \cdot (C_2H_5NH_3)SbCl_4$ has been determined at 295 K. It is the first example, in the group of halogenoantimonates(III) and bismuthates(III), of a salt of $R_4M_3X_{13}$ stoichiometry (R-cation, M = Sb, Bi, X = Cl, Br, I). The crystal structure of the title compound is composed of two independent $(Sb_2Cl_9^{3-})_n$ and $(SbCl_4^-)_n$ polyanionic zig-zag chains and four crystallographically non-equivalent ethylammonium cations.
- $(C_2H_5NH_3)_3Sb_2Cl_9 \cdot (C_2H_5NH_3)SbCl_4$ has been studied by DSC, dielectric and thermal expansion methods. A phase transition at T_c = 274 K of first order and the order-disorder type has been

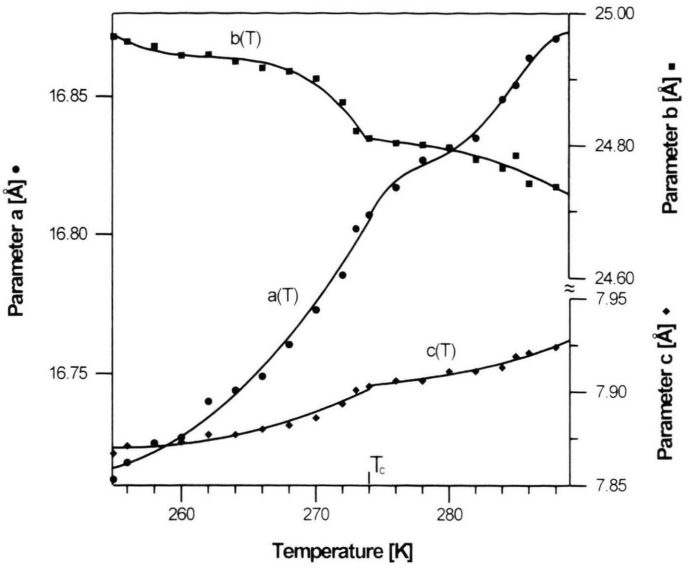

Fig. 6. Temperature dependence of the *a*, *b* and *c* lattice parameters of $(C_2H_5NH_3)_3Sb_2Cl_9 \cdot (C_2H_5NH_3)SbCl_4$. The curves were fitted for two phases, below and above T_c, using the least-squares method.

found. The mechanism of the phase transitions is most probably connected with the freezing of the reorientation motions of at least one out of three disordered at room temperature crystallographically non-equivalent ethylammonium cations.

Acknowledgement

This work was partly supported by the Polish State Committee for Scientific Research (project register No. 3 T09A 104 17).

[1] J. Zaleski, R. Jakubas, L. Sobczyk, and J. Mróz, Ferroelectrics **103**, 83 (1990).
[2] R. Jakubas, L. Sobczyk, and J. Matuszewski, Ferroelectrics **74**, 339 (1987).
[3] G. Bator, R. Jakubas, L. Sobczyk, and J. Mróz, Ferroelectrics **141**, 177 (1993).
[4] R. Jakubas, Z. Galewski, L. Sobczyk, and J. Matuszewski, Ferroelectrics **88**, 83 (1988).
[5] U. Ensinger, W. Schwarz, and A. Schmidt, Z. Naturforsch. **37b**, 1584 (1982).
[6] M. Bujak and J. Zaleski, Polish J. Chem. **73**, 773 (1999).
[7] P. Ciąpała, J. Zaleski, G. Bator, R. Jakubas, and A. Pietraszko, J. Phys. Condens. Matter. **8**, 1957 (1996).
[8] U. Ensinger, W. Schwarz, and A. Schmidt, Z. Naturforsch. **38b**, 149 (1983).
[9] G. M. Sheldrick, SHELXTL Siemens Analytical X-ray Instruments Inc., Madison, Wisconsin, USA (1990).
[10] KUMA, KUMA Diffraction Software, version 8.1.0 and 8.1.1. KUMA Diffraction, Wrocław, Poland (1996).
[11] G. M. Sheldrick, SHELX-97. Program for Solution and Refinement of Crystal Structure University of Göttingen, Germany (1997).
[12] L. Pauling, The Nature of the Chemical Bond, Cornell University Press Ithaca, N. Y. (1960).